Climate driven history of Holocene erosion in Eastern Europe- the example of a catchment at a giant Chalcolithic settlement at Maidanetske, central Ukraine

Stefan Dreibrodt*[1], Robert Hofmann[2], György Sipos[3], Lorenz Schwark[4], Michail Videiko[5], Liudmyla Shatilo[2], Sarah Martini[1], Philipp Saggau[6], Rainer Duttmann[6], Hans-Rudolf Bork[1], Wiebke Kirleis[2], Johannes Müller[2]

*-- corresponding author: sdreibrodt@ecology.uni-kiel.de

1, Institute for Ecosystem Research, CRC 1266, University of Kiel, Germany

2, Institute for Pre- and Protohistoric Archaeology, CRC 1266, University of Kiel, Germany

3, Department of Physical Geography and Geoinformatics, University of Szeged, Hungary

4, Institute of Geoscience, CRC 1266, University of Kiel, Germany

5, Laboratory of Archaeology, Borys Grinchenko Kyiv University, Ukraine

6, Department of Geography, CRC 1266, University of Kiel, Germany

Abstract

The younger Quaternary erosion history was reconstructed in a catchment close to the Chalcolithic giant settlement Maidanetske, central Ukraine based on dated sediment sequences. Four trenches and a long percussion drill-core were analyzed in a valley grading from a Loess covered plateau towards the Talianky River. The sediments were dated via a combination of radiocarbon dating, optical stimulated luminescence (OSL) and embedded artefacts. A suspicious non-coincidence between phases of soil erosion and the settlement history at the site over long periods of the Holocene is noticeable and suggests a climatically driven erosion at the site. The detected phases of erosion during the past >20,000 years coincide with global (cal 27.6 +/- 1.3 kyrs BP, 12.0 +/- 0.4 kyrs BP), northern hemispheric (cal 8.5 ± 0.3 kyrs BP), Mediterranean (cal 3.93 ± 0.1 kyrs BP) as well as western to central European (2,700 to 2,000 cal BP) climate anomalies. For these anomalies, characterized by colder than usual conditions in western and central Europe and dry conditions in the eastern Mediterranean and the research area, a common trigger process seems possible. Increased occurrences of heavy precipitation events, probably during phases of a weakened vegetation cover, could explain the observed record.

A comparison of the Ukrainian record with other European erosion records raises the question again about the contribution of climate variability on Holocene erosion processes. Whereas climatic influence might be easier detectable in Eastern Europe, with a comparatively late onset of intensive agricultural land use, in southern, central and western Europe the impact of climate variability might be masked to a part according to the long history of intensive agricultural land use.

The composition of the sediments implies changes of the slope-channel connectivity during the deposition history. Whereas the periglacial to early Holocene sediments were derived from the whole catchment area, since the mid-Holocene a tendency to lower slope storage of colluvial material and valley incision is noticeable.

Keywords: Holocene Erosion, climate and land-use, Ukraine, connectivity

1. Introduction

Based on numerous geomorphological investigations in southern and central Europe soil erosion has been identified as one of the major and most serious impacts of humanity on the environment (e.g. van Andel et al., 1990, Bork and Lang 2003, Butzer, 2005, Dotterweich, 2008, Thornes, 2009, Dreibrodt et al., 2010a). Within the research region, few data about the younger Quaternary and Holocene geomorphological processes at the slope scale are available. Without giving information about the land use history of the catchment area Belyaev et al. (2004) report phases of gully activity in small catchments in western Russia at ca. cal BP 1090-970 and 880-570. Similarly, without information about Holocene land use history, Belyaev et al. (2005) report gully activity at two additional sites in western Russia at ca. cal BP 8,950-8,480, 4,100-3,400, 3,140-2,870, 2,310-2,170, 1,590-1,031, and 640-490. Panin et al. (2009) found a pre-Holocene origin of 15 of 19 studied gully systems in western Russia. During the Holocene, these authors detected longer phases of erosion and gully activity from ca. 4,800 to 2,800 cal BP and 1,200 cal BP until today. Shorter periods of intenisve erosion were reconstructed for the intervals ca. 4,800- 4,600, 3,900-3,600, 3,800- 2,800, 2,300- 2,100, 1,600-1,800, 1,000-800, and 700-500 cal BP. The phases of erosion were explained mainly by climate variability. Sycheva (2006) and Sycheva et al. (2003) report a quasi-cyclicity of erosion and soil formation at the Russian part of the East European Plain based on a compilation of radiocarbon dates form soils and slope deposits. The observed cyclicity is ascribed to periodical climatic changes throughout the Holocene. Intervals of intensive soil erosion were dated to ca. 10,200-9,500, 8,100-7,700, 6,600-6,300, 4,700-4,200, 2,700-2,300, and 950-450 cal BP. Whereas researchers from southern and central Europe underline the role of agricultural land use on soil erosion histories of the respective landscapes, eastern European scholars rather see climatic variability and their effects on vegetation as the main drivers of Holocene relief change. Thus, a comparison of the land use history known from intensive archaeological research with the detectable phases of soil erosion at the research site is one focus of this paper.

2. Material and methods

2.1 The research site

The investigated catchment area is located at Majdanetskoe, district of Talne, central Ukraine (48°48′N, 30°38′E) (Fig. 1). The close by archaeological site of Madanestske is a giant settlement of the Tripyllia C1-period (Müller et al., 2013, 2016, Hofmann et al., 2019). Archaeological sites of this type are unique because of their extremely large dimensions. At Maidanetske, on an area of 200 ha approximately 3,000 houses arranged in a series of oval structures around an unbuilt central space were inhabited approximately from 3,990 to 3,640 BCE (Müller et al., 2016, Ohlrau, 2018, Pickartz et al., 2019). Surveys of the many potshards present on the recent surface, magnetic surveys, excavations and exhaustive dating campaigns revealed a maximum number of ca. 1,500 houses was inhabited contemporaneously by probably more than 10,000 people (Ohlrau, 2018, Pickartz et al., 2019). The climate in the region is humid continental (Dfb) today, with hot summers and cold wet winters. The potential natural vegetation of the region belongs to the climate sensitive forest-steppe transition zone. Where there is no agricultural land use, deciduous forests are present in the landscape today. A mosaic of loess-covered plateaus dissected by small valleys characterizes the recent topography. The surface soils are classified as particularly thick Chernozems in the research area (Atlas of soils of the Ukrainian SSR, 1979). The studied catchment area covers ca. 6.3 km² and grades from a Loess plateau towards the valley of the Talianky River spanning a relief gradient from ca. 210 to 150 m a.s.l. Ditches and a small pond subdivide the valley nowadays. Meadows and shrubs cover parts of the valley. The catchment area is used for large agricultural fields, subdivided by wind-breaking tree lines, ditches and unpaved roads.

2.2 Methods

2.2.1 Field methods

Five trenches were dug at the lower slopes of the catchment area of the investigated valley (Fig. 1). Additionally, a sediment sequence was extracted from a long (5m) percussion-drilling core situated on the colluvial fan of the investigated valley close to its outlet into the larger valley of the Talianky River.

The sequences of soils and sediments were documented in scaled drawings and described according to field instructions (AG Boden, 2005). Sediments are termed as slope deposits (abbr. S) respectively colluvial layers (abbr. M), if they are of pre-Holocene respectively Holocene age and numbered in the order of their genesis. Samples were taken for dating and standard laboratory analyses.

2.2.2 Laboratory analysis

Dating

Dating of the soils and sediments was achieved through radiocarbon measurements, optical stimulated luminescence (OSL) and typological analysis of embedded artifacts. Given the scarcity of datable bioremains, radiocarbon dating of bulk samples soil organic matter samples was performed after removal of carbonates. The results were calibrated using OxCal v4.2.3 (Bronk Ramsey and Lee, 2013) with the IntCal13 atmospheric calibration curve (Reimer et al., 2013) and are presented in cal years BP (2 Sigma). OSL dating was carried out on unexposed samples taken in small tubes in exposure 2 and from segments of a parallel core from drilling point 1. A RISO TL/OSL DA-15 luminescence reader equipped with a calibrated 90Sr/90Y source was used for measurements. Stimulation was carried out using blue (470 nm) or IR (870 nm) LEDs, depending on the applied mineral fraction. Detection was made through either a U-340 filter (quartz) or the combination of BG39 and CN-7-59 filters (feldspar). Throughout the measurements different types of the Single Aliquot Regeneration (SAR) protocol was used (Murray and Wintle, 2000, 2003, Wintle and Murray, 2006, Thiel et al., 2011, Buylaert et al., 2012). Prior to the measurement of the equivalent dose (De) tests were carried out to determine optimal temperature parameters and the reproducibility of the

SAR procedure (combined preheat and dose recovery test). The equivalent dose was determined on several aliquots in case of each sample. Only those aliquots were considered for De calculation which passed the following rejection criteria (recycling ratio: 1.00±0.10; maximum dose error: 10%; maximum recuperation: 5%, maximum IR/OSL depletion ratio: 5%). Sample De was determined on the basis of each accepted aliquot De, using different statistical techniques (Galbraith et al., 1999). Decision was made on the basis of over dispersion, skewness and kurtosis values. Environmental dose rate D* was determined using high resolution, extended range gamma spectrometer (Canberra XtRa Coaxial HpGe detector). Dry dose rates were calculated using the conversion factors of Liritzis et al. (2013). Wet dose rates were assessed on the basis of in situ water contents. The dose rate provided by cosmic radiation was determined on the basis of the geographical position and depth of the samples below ground level, using the equation of Prescott and Hutton (1994). All OSL ages given in the text and figures of this paper are given in cal years BP (1 Sigma). Artifacts embedded in soil or sediments were dated according to prevailing typochronologies by the archaeologists. All radiometric age data are given completely in Table 1a and 1b.

Geophysical and geochemical analysis

Soil and sediment samples were air dried (35°C), carefully disintegrated with mortar and pestle and sieved through a 2 mm mesh sieve.

Grain size distribution analysis was carried out for profiles 2, 3, and the sediment core 1. After removal of soil organic matter (H_2O_2, 70 °C) and carbonates (acetic acid buffer, 70°C, pH 4.8) a laser particle sizer (Malvern Mastersizer 2000) was used to measure the grain size distribution (core1, profiles 2 and 3). Each sample was measured for at least 45 seconds, and the measurement was repeated at least 10 times, and finally averaged. The magnetic susceptibility was measured on 10 ml samples (< 2 mm fraction) using a Bartington MS2B susceptibility meter (resolution $2*10^{-6}$ SI, measuring range 1-9999$*10^{-5}$ SI, systematic error 10 %). Measurements were carried out at low (0.465 kHz) and high (4.65 kHz) frequency. A 1 % Fe_3O_4 (magnetite) was measured regularly to check for drift and calibrate the results. Mass-specific susceptibilities and frequency-dependent magnetic susceptibility (χfd) were calculated (Dearing, 1999). The color of the samples was measured using a Voltcraft Plus RGB-2000 Color Analyzer set to display in a 10-bit RGB color space within a spectral range of 400 to 700 nm (Rabenhorst et al., 2014, Sanmartin et al., 2014). Loss on Ignition (LOI) values were measured as estimates of the organic matter and carbonate content of the sediments (Dean, 1974). After drying the samples at 105°C overnight, the weight loss of the samples was determined after heating times of 2 h at 550 °C and 940 °C each. For selected profiles, some additional analysis was carried out. The total carbon (TOC), total nitrogen (TN) were determined with an Elementar Vario EL-III CNS analyser following standard procedures. Sulfanic acid (S= 18.5 weight %) was used for instrument calibration and an analytical error of ± 0.01 % was determined. On selected samples from the soil and sediment sequence of core 1 a lipid analysis was carried out to infer about the catchment vegetation. Lipids were extracted using pressurized liquid Extraction (DIONEX ASE200) using a solvent mixture of hexane/dichloromethane (9/1; v/v) and separated into non-polar and polar compound classes by automated SPE (LC-Tech Freestyle) on 2 grams of pre-extracted and activated silica. Non-polar compounds were eluted with hexane/dichloromethane (9/1; v/v) and subjected to gas chromatography-mass spectrometry (GC-MS) using an Agilent 7890A GC equipped with a Phenomenex Zebron ZB-5 column (30m × 0.25mm i.d.; 0.25 µm film thickness) and coupled to an Agilent 5975B mass chromatograph. The injection temperature was held at 60°C for 4 min, after which the oven temperature was raised to 140°C at 10°C/min and subsequently to 320 °C at 3°C/min, at which it was held for 8 min. The MS was operated at an electron energy of 70 eV and an ion source temperature of 250°C. The homologues series of n-alkanes was detected via the m/z 85 mass chromatograms and peak areas used for calculation of relative abundance ratios.

3. Results

Deposition history

Sequences of sediments deposited during the younger Quaternary and soils that had formed within these sediments during phases of slope stability were detected at the different exposures (Fig. 1) and at the drilling point (Fig. 2).

Sediment core 1

At the drilling point on the colluvial fan of the investigated valley, the thickest sediment sequence (ca. 5m) was recovered (Fig. 2). The base layer S1 (4.4- > 5.0 m) comprises of a larger amount of gravel (ca. 4.7- > 5.0 m) and sand of a light greyish color and dates to the LGM according to an OSL datum. Above, a layer of Loess was deposited (S2, ca. 4.0- 4.4 m). This pale yellowish layer is composed mainly of silt with some sand and clay admixed. It is unclear so far, whether S2 originated from aeolian deposition or is a fluvial redeposition. S2 dates to a period between the LGM and the YD. A YD fluvial sediment was detected above (S3, 3.3- 4.0 m). Its dark brown color and silty texture (finer than the lying Loess) points to an Allerød soil within the catchment as the source of the sediment. An OSL age, backed by a radiocarbon age of the soil organic matter, pointing to a deposition of S3 at ca. 12.0 +/- 0.4 ka BP. S3 was buried by an early Holocene deposit M1 (3.0- 3.3m). Although the texture of M1 again is comprised mainly of silt, a significant switch towards finer silt particles implies a change in the depositional conditions. The still dark brownish color indicates that the source of M1 was an early Holocene soil that covered the catchment area. According to an OSL age, the deposition of M1 occurred at 8.5 +/- 0.3 ka BP. A radiocarbon age of soil organic matter from the layer is slightly younger (ca. 8.160- 7880 cal BP, 2 Sigma). Additional radiocarbon ages from the upper part of M1 imply that a soil has formed after the deposition of the sediment. The numerical data suggest that this soil formation started by ca. 5,900 cal BP (2 Sigma). M1 was buried by M2 at ca. 3.93 +/- 0.3 ka BP according to an OSL age (backed by a radiocarbon age of soil organic matter). M2 (1.95- 3.0 m) has a slightly paler color (dark grayish brown), and, while still dominated by silt, a significant increase in sand (coarse and middle sand). In the upper part of M2 another soil has formed from ca. 2,750 cal BP until it became buried by M3. Whether M3 was deposited during Iron Age or Medieval Times is not clear due to sparse numerical age information. Data from the other exposures within the catchment area point to the former. Changes in the sediment composition could be used to subdivide M3. A change in sediment color (darker), grain size (little sand), and the C:N ratio of the sediment indicates a former soil surface (A-horizon, soil formation) in a depth of ca. 1.5 m, coinciding with a radiocarbon age of ca. 910- 730 cal BP (Medieval Times). Another noticeable change of the sediment properties is visible in ca. 1.0 m depth. Similarly, few sand, additionally higher clay content, a switch to darker sediment colors and wider C:N ratios indicate another former surface horizon (A-horizon, soil formation). Thus, although not dated numerically the deposition of an Iron Age colluvium followed by two subsequent colluvial layers could be derived from the sediment properties.

The $nC_{27}/(nC_{27+31})$ plant wax alkane ratio of the sediment indicates increasing amount of tree leaves within the soil organic matter comparing the Late Glacial to mid-Holocene sediment record. It is the smallest in one YD sample, increases in the samples of the early Holocene layer, and further to a more tree-dominated value in the mid-Holocene samples.

Trenches at the lower slopes

At the lower slopes that incline towards the studied valley (trenches 2, 3, 5, 6), varying but smaller thicknesses of sediments of water erosion were exposed (Fig. 1, 2; between 1-2 m). All sediments are composed of silt, clay, and fine sand, and containing no significant amount of coarser particles. There are different occurrences of Late Glacial to early Holocene sediments (trenches 2, 3). In one trench, a thin Early Bronze Age colluvium was detected (trench 3). All trenches contain a colluvial layer that dates to ca. 4,000 cal BP. In two trenches, the presence of a sediment deposited ca. 2,700- 2,300 yrs cal BP (trenches 2, 5) is proven. In all trenches, spurs of buried soils are present. At the base of the trenches, remnants of a buried Bw-horizon (Cambisol) indicate the presence of a wooded landscape prior to the nowadays-widespread Chernozems. Additionally, pronounced A-horizons subdivide the sediment sequences indicating a succession of alternating phases of slope stability and erosion throughout the younger Quaternary. Within the YD sediment deposited at trench 2, a humic surface soil horizon has formed dating to ca. 5,900- 5,650 yrs cal BP. In trench 3, similar phases of soil formation are indicated. These occurred in the upper part of the early Holocene colluvial layer at ca. 7,800-7,600 yrs cal BP until burying at ca. 5,000- 4,900 yrs cal BP and in the colluvial layer suspicious to have been deposited at ca. 4,000 yrs BP at ca. 3,900-3,700 yrs cal BP until burying at ca. 3,000- 2,900 yrs cal BP.

In general, the sediments and soils exposed at the lower slopes resemble the chronostratigraphy detected in the long percussion-drilling core at the colluvial fan. Fig. 2 b and c illustrate properties of the deposited sediments and soils in the trenches 2 and 3. Noteworthy is the comparable similar grain size distribution (mainly silt with some clay) in trench 2 and 3. This might be explained by their delivering sediment sources comprising of Loess at the investigated slopes. While there are similar trends in LOI, magnetic susceptibility and colors of the sediment sequences in trench 2 and 3, there is an obvious difference at the base of the Holocene part of the sequences. All, the LOI 940 values, the magnetic susceptibility and the colors in trench 2 show an abrupt step at this chronostratigraphical border whereas there is a gradual transition in trench 3. This indicates an erosional discordance in trench 2 between the Late Glacial and the mid-Holocene. Erosion of parts of the soil developed in the Late Glacial deposit immediately before the onset of soil formation (ca. 5,900- 5,650 yrs cal BP) seems the most probable reason for the observed data.

An additional exposure was studied in a small quarry ca. 3 km southwest of the investigated catchment area (trench 4). Whereas the start of erosion was found to have happened ca. 3,700- 3,500 yrs cal BP, the subsequent colluvial layer dates to ca. 2,700- 2,400 yrs cal BP, resembling an erosional phase detected in the investigated valley. A pronounced buried Bw-horizon is present at the base of the sequence.

4. Discussion

A comparison of the reconstructed phases of erosion and soil formation with the well known settlement history of the region and Holocene erosion histories from the Russian Plain and Germany is given in Fig. 3. The data from the investigated trenches and the percussion-drilling core indicate that the younger Quaternary erosion at the sites occurred in discrete phases. Slight deviations between datings can be ascribed to uncertainties in using bulk samples for radiocarbon dating. A comparison with the settlement history, thoroughly investigated through extensive archaeological surveys and excavations near the research area shows a conspicuous non-coincidence between land-use and erosion history. The only noticeable exception is the last millennium, where we do not have numerical age information about the sediment deposition. No traces of erosion were found to be related with the phases with the largest number of prehistoric settlements in the area (20 km radius) at ca. 6,450-5,350 yrs cal BP (Tripyllia culture) or at ca. 1,700-1,500 yrs cal BP (Late Roman Iron Age). This strengthens the opinion of a group of eastern European geomorphologists that Holocene erosion in Eastern Europe was mainly driven by climate variability (Sycheva et al., 2003, Belyaev et al. 2004, 2005, Sycheva 2006, Panin et al. 2009). A comparison of the numerical ages of the detected erosion phases reveals a weak accordance between the results from central Ukraine and the Russian Plain for some erosion phases. Whereas the records from Russia show no pronounced consistence viewed by itself, the erosion phases at ca. 8.0 kyrs BP, ca. 4,000 yrs cal BP, at ca. 2,700-2,300 yrs cal BP and during the last millennium detected in central Ukraine are also visible in the Russian record.

Considering them separately, all erosion phases detected at Maidanetske coincide with periods of known extreme climatic conditions or rapid climate variability.

An in generally cooler and drier than today environment has been reconstructed for the LGM (e.g. Lowe et al., 2008). Large regions of the non-glaciated forelands were characterized by permafrost (e.g. Renssen and Vandenberghe, 2003), leading to increased amounts of runoff during summer thawing or precipitation events (Panin et al., 2009). This resulted in widespread increased erosion processes as described for the Mediterranean (Rossato and Mozzi, 2016) or Russia (Panin et al. 2009). Of 19 gullies studied by Panin et al. (2009) in central Russia 15 were incised initially already during the Pleistocene. The deposition of a sediment in the sequence of Maidanetske, rich in stones and sand, at 26.5 +/- 0.7 ka cal BP could have been related to an intense runoff event on partly frozen ground. Its coarse texture might reflect high runoff energy and resulting incision of gullies/ channels into the bedrock. Loess contributed, if even, only a small amount to the sediment.

The YD climate oscillation is well studied in a large number of palaeoenvironmental archives (e.g. Bar-Matthews et al., 1997, Brauer et al., 2001, Andersen et al., 2004, Dykoski et al., 2005, Staubwasser and Weiss, 2006, Bordon et al., 2009) and characterized as a cold and dry phase across Europe. Slope instability associated with abrupt climate change has been reported from various sites in Europe (e.g. Andres et al., 2001, Dotterweich et al., 2013) or Anatolia (e.g. Dreibrodt et al., 2014). Regardless if permafrost processes affected the research region during the YD, the vegetation cover and thus the shelter of the surface soil was very probably affected by climate change. These conditions could explain the observed erosion phase in central Ukraine by runoff events produced during water rich snow-melts or intensive precipitation events on unsheltered surface soils. The layers detected at two points in the sedimentation area contain a large amount of silt, indicating the presence of a Loess cover in the catchment area that was not cut through by the erosion processes.

The detection of a slope instability phase at ca. 8,000 yrs cal BP coincides with another well-known climate oscillation phase (e.g. Alley and Ágústsdóttir, 2005). Response to this phase of rapid climate change has been reported widespread from different types of palaeoenvironmental archives, such as lakes (e.g. Migowski et al., 2006, Prasad et al., 2007, Bordon et al., 2009), tree rings (e.g. Spurk et al., 2002), or speleothems (e.g. Bar-Matthews et al., 1997, Bar-Matthews and Ayalon, 2011). While it is accepted that the 8 ka BP phase was related to cold conditions in the northern mid-latitudes its hydrologic impact is less clear. In spite of few evidence for flooding (e.g. Macklin et al., 2006) most researchers interpret the occurrence of slope instability as a result of wetter conditions (e.g. Zolitschka and Negendank, 1998). However, dry spells, which led to a destruction of the vegetation cover (wildfires), might provide an alternative reason for slope instability (e.g. Dreibrodt et al. 2010b). Since lake level highstands were used as an additional argument for wetter conditions across western and central Europe (e.g. Magny et al., 2003) it might be considered that both, colder temperatures and a sparser vegetation cover in the lakes catchment might also result in lake level increases. From the eastern Mediterranean, there is indication for drier climate conditions at around 8,000 cal BP (e.g. Bar-Matthews et al., 1997, Migowski et al., 2006, Bar-Matthews and Ayalon, 2011). Some scholars even argued about a close relationship between the climate anomaly and early societal evolution in the Mediterranean (Weninger et al., 2006). Investigations on slope deposits have revealed a pronounced phase of slope instability at this interval reported from sites as distant as western and central Europe (e.g. Dreibrodt et al., 2010b, Vincent et al., 2010, Lubos et al., 2011, Schumacher et al., 2018) or Anatolia (Dreibrodt et al., 2014). The 8.0 ka climate oscillation is considered to have been of smaller amplitudes in temperature and moisture changes as well as duration compared with the YD phase. Effects of permafrost or enduring changes of the vegetation cover are less probable to explain the observed erosion in central Ukraine. A weakened vegetation cover could have well played a role, but an accentuation of patterns of precipitation events is also quite possible.

The erosion phase at ca. 4,000 yrs cal BP coincides with a climate anomaly reported from different sites across Eurasia. Whereas northern Europe and the Alps experienced a colder than usual phase (e.g. Bakke et al., 2010, Le Roy et al., 2017) from southern Europe and the Mediterranean the climate oscillation is rather known because of prominent drought phases (e.g. Weiss and Bradley, 2001, Staubwasser and Weiss, 2006, Migowski et al., 2006, Cheng et al., 2010, Schirrmacher et al., 2019). A prominent dry phase was also reconstructed from the lake level of Lake Balqash (Kremenetski, 1997) and through pollen studies for the research region in the period from ca. 4,300 to 3,600 yrs cal BP (Gerasimenko, 1997). Intensive erosion during the period was detected in Greece (e.g. van Andel et al., 1990) or Anatolia (Dusar et al., 2014). Thus, accentuated precipitation events during an in general drier than usual phase with a weakened vegetation cover, could explain the erosion phase detected at Maidanetske.

Between ca. 2,700 and 2,300 yrs cal BP another erosion phase occurred at Maidanetske. This coincides with a climatic deterioration phase recorded across western and central Europe (e.g. van Geel et al., 1996). Prominent dry conditions were reconstructed for ca. 3,000- 2,000 cal BP from marine sediments of the eastern Mediterranean (Schilman et al., 2001) and for the period between ca. 2,700- 2,000 cal BP from the lake level of Lake Balqash (Kremenetski, 1997). Pollen studies from the research region indicate a drier than usual phase from ca. 3,000 to 2,400 yrs cal BP (Gerasimenko, 1997). In central Europe, frequent erosion has been reported from a large number of sites during this period (e.g. Lang, 2003, Dreibrodt et al., 2010a), including phases of gullying (Dreibrodt and Wiethold, 2015). Note the presence of a high number of colluvial layers deposited in Germany in the period between 2,700 to 2,300 yrs cal BP (Fig. 3). Erosion is reported during the period from Anatolia (Kaniewskie et al., 2008, Dreibrodt et al., 2014, Dusar et al., 2014) and Greece (van Andel et al., 1990, Fuchs, 2007), additionally. Thus, accentuated precipitation events during a generally drier than usual phase with a weakened vegetation cover, could explain the erosion phase detected at Maidanetske.

Since we do not have numerical age information about the erosion processes that were in action during the past millennium at Maidanestke, we can only state that this phase was the strongest influenced by intensive agricultural land use at the research site. Maxima of erosion are reported from central Europe (e.g. Bork and Lang, 2003, Dotterweich, 2008, Dreibrodt et al., 2010a) and Russia (Panin et al., 2009) to have happened during this period. If we consider the record at the colluvial fan in core 1 we could deduce that about 150 cm of the Holocene record was deposited during the last 1,000 years (representing ca. 42 % of the Holocene sediment). That underlines again the crucial importance of intensive agricultural land use on Holocene soil erosion processes. Additionally, it implies that the intensity of prehistoric land use was below a critical threshold, thus no or very little soil erosion was triggered by their subsistence systems.

Summarizing the discussion of the long-term Younger Quaternary erosion history at Maidanetske (LGM- 1,000 yrs BP) there is a non-coincidence of erosion with the local and regional settlement history but an obvious pattern of coincidence of erosion at the site with well-known phases of climate anomalies. The latter reflect anomalies reported from western and central Europe and the Mediterranean climate system. Their visibility in central Ukraine might reflect the convergence of the two climate systems in that part of Eastern Europe. As the climate anomalies conspicuous to have resulted in the observed erosion were characterized by similar conditions (colder than usual in central and western Europe and drier than usual in the eastern Mediterranean and the research area) a common trigger of the observed erosion phases might be possible. Episodic occurrences of more intensive than usual precipitation events in the research area one a perhaps weakened vegetation could explain the observed record. This is corroborated by the accordance of dating of sediment layers at the different investigation points that implies discrete phases of Holocene erosion. A response of the local vegetation cover to slight climatic changes seems probable considering the position of the site in the sensitive ecotone of the forest-steppe transition. If occurrences of heavy precipitation events coinciding with the climate anomalies were triggered by short response mechanisms of the climate system as occurrences of meridional transfer of heat and water from the eastern Mediterranean towards the interior of Eurasia remains speculative and is a matter of ongoing research.

The sensitivity of the central Ukrainian landscape we claim here is probably related to two preconditions. The first is the late onset of intensive agricultural land use in the region, similar as pointed out for Russia (Panin et al., 2009). This is visible in the thick layer of colluvial material deposited during the last millennium in our long percussion-core. The second precondition is related to the location of the area in the forest-steppe borderland zone, considered to be sensitive to slight climatic changes and, additionally located in a position where western and southern European climate systems converge.

Considering the erosion processes in action during the Younger Quaternary deposition history an additional observation could be made. The sediment deposited during the periglacial to early Holocene erosion processes show properties that resemble the Loess cover deposited over the whole catchment area (Fig. 2). Since the 4,000 yrs cal BP erosion phase, the sediment on the colluvial fan contains more sand in general. This is not visible in the trenches at the lower slopes, where the Loess cover was nowhere found to have been cut through completely. This hints to the start of a stronger incision in the valley itself and aggradation of colluvial material at the lower slopes. Additionally, the biomarker signal of increasing amounts of tree leave organic matter in the valley sediments points to erosion and redeposition of soil in the valley bottom, because the valley bottom is the most probable place for the growth of gallery forests throughout the Holocene. Thus, a change in the overall geomorphic connectivity within the investigated catchment area occurred at the mid-Holocene (since 4,000 yrs cal BP). This could reflect changes in the intensity of the reconstructed erosional events in an order (from stronger to weaker): LGM > YD > early Holocene >> mid-Holocene.

5. Conclusions

A long-term Younger Quaternary erosion history mainly driven by climate variability was reconstructed at a central Ukrainian site. This is in accordance with observations from neighboring regions. It might reflect the late onset of intensive agricultural land use in the region and the position of the site in an environment sensitive to slight climatic shifts where the western and southern European climate systems converge. Additionally, in western, central and southern European records of Holocene erosion response to climate variability might be present but masked by the anthropogenically intensified erosion of early intensive land use.

Changes in the properties of the sediment deposited at a colluvial fan indicate a change from a stronger connectivity of erosion processes during the glacial to early Holocene erosion phases towards a weakened connectivity since the mid-Holocene (4,000 yrs cal BP).

Acknowledgements

We are grateful to the DFG for funding in the frame of the CRC 1266 “Scales of transformation”. Many thanks to the landowners for allowance of the fieldwork, and Imke Meyer, Manfred Beckers, Tine Karck, Katie Lehnen, and a group of students of the University Kiel for help in the laboratory.

References

AG Boden, 2005. Bodenkundliche Kartieranleitung. 5. verbesserte und erweiterte Aufl. Schweizerbart'sche Verlagsbuchhandlung, Stuttgart.

Alley, R.B., Ágústsdóttir, A.-M., 2005. The 8k event: cause and consequences of a major Holocene abrupt climate change. Quaternary Science Reviews 24, 1123–1149.

Andersen, K.K., Azuma, N., Barnola, J.M., Bigler, M., Biscaye, P., Caillon, N., et al., High-resolution record of Northern Hemisphere climate extending into the last interglacial period. Nature 431, 147-151.

Andres, W., Bos, J.A.A., Houben, P., Kalis, A., Nolte, S., Rittweger, H., Wunderlich, J., 2001. Environmental change and fluviual activity during the Younger Dryas in central Germany. Quaternary International 79, 89–100.

Atlas of Soils of the Ukrainian Socialistic Soviet Republic, 1979. Harvest, Kiew.

Bakke, J., Dahl, S.O., Paasche, O., Riis Simonsen, J., Kvisvik, B., Bakke, K., Nesje, A., 2010. A complete record of Holocene glacier variability at Austre Okstindbreen, northern Norway: An integrated approach. Quaternary Science Reviews 19, 1246-1262.

Bar-Matthews, M., Ayalon, A., 2011. Mid-Holocene climate variations revealed by high-resolution speleothem records from Soreq Cave, Israel and their correlation with cultural changes. *The Holocene* 21(1), 163–171.

Bar-Matthews, M., Ayalon, A., Kaufman, A., 1997. Late Quaternary palaeoclimate in the eastern Mediterranean region from stable isotope analysis of speleothems at Soreq Cave, Israel. *Quaternary Research* 47: 155–168.

Belayev, Y.R., Panin, A.,V., Belayev, V.,R., 2004. Climate-induced and local-scale erosion and sedimentation features in small catchments: Holocene history of two small valleys in Central Russia. Sediment Transfer through the Fluvial System, IAHS Publ. 288, 3-12.

Belayev, V.R., Eremenko, E.A., Panin, A.V., Belayev, Y.R., 2005. Stages of Late Holocene gully development in the central Russian plain. International Journal of Sediment Research 20, 224-232.

Bordon, A., Peyron, O., Lézine, A.-M., Brewer, S., Fouache, E., Pollen-inferred Lat-Glacial and Holocene climate in southern Balkans (Lake Maliq). Quaternary International 200, 19-30.

Bork, H.-R., Lang, A., 2003. Quantification of past soil erosion and land use/ land cover changes in Germany. In: Lang, A., Hennrich, K., Dikau, R. (Eds.), Long Term Hillslope and Fluvial System Modelling: Concepts and Case Studies from the Rhine River Catchment. Springer, Heidelberg, pp. 231-239.

Brauer, A., Litt, T., Negendank, J.F.W., Zolitschka, B., 2001. Lateglacial varve chronology and biostratigraphy of lakes Holzmaar and Meerfelder Maar, Germany. Boreas 30, 83–88.

Bronk Ramsey, C., Lee, S., 2013. Recent and planned developments of the program OxCal. *Radiocarbon* **55,** 3–4.

Butzer, K.W., 2005. Environmental history in the Mediterranean world: cross-disciplinary investigation of cause-and-effect for degradation and soil erosion. Journal of Archaeological Science 32, 1773-1800.

Buylaert et al., 2012. A robust feldspar luminescence dating method for Middle and Late Pleistocene sediments. *Boreas* **41**, 435–451.

Cheng, H., Sinha, A., Verheyden, S., Nader, F.H., Li, X., Peng, Y.B., Rao, Z.H., Ning, Y.F., Edwards, R.L., 2015. The climate variability in northern Levant over the past 20,000 years. Geophysical Research Letters 22, 8641-8650.

Dean, W.E., 1974. Determination of Carbonate and Organic Matter in Calcareous Sediments and Sedimentary Rocks by Loss on Ignition: Comparison with Other Methods. *Journal of Sedimentary Petrology* **44,** 242–48.

Dearing, J., 1999. *Environmental Magnetic Susceptibility: Using the Bartington MS2 System*. 2nd ed. (Bartington Instruments Ltd.).

Dotterweich, M., 2008. The history of soil erosion and fluvial deposits in small catchments of central Europe: deciphering the long term interaction between human and environment – a review. Geomorphology 101, 192–208.

Dotterweich, M., Kühn, P., Tolksdorf, J.F., Müller, S., Nelle, O., 2013. Late Pleistocene to Early Holocene natural and human influenced sediment dynamics and soil formation in a 0-order catchment in SW-Germany (Palatinate Forest), Quaternary International 306, 42-59.

Dreibrodt, S., Wiethold, 2015. Lake Belau and its catchment (northern Germany): A key archive of environmental history in northern central Europe since the onset of agriculture. The Holocene 25(2), 296–322.

Dreibrodt, S., Lubos, C., Terhorst, B., Damm, B., Bork, H.-R., 2010a. Historical soil erosion by water in Germany: Scales and archives, chronology, research perspectives. *Quaternary International* 222, 80–95.

Dreibrodt, S., Lomax, J., Nelle, O., Lubos, C., Fischer, P., Mitusov, A., Reiss, S., Radtke, U., Nadeau, M, Grootes, P.M., Bork, H.-R., 2010b. Are mid-latitude slopes sensitive to climatic oscillations? Implications from an Early Holocene sequence of slope deposits and buried soils from eastern Germany. *Geomorphology* 122, 351–369.

Dreibrodt, S., Lubos, C., Lomax, J., Sipos, G., Schroedter, T., Nelle, O., 2014. Holocene landscape dynamics at the tell Arslantepe, Malatya, Turkey – Soil erosion, buried soils and settlement layers, slope and river activity in a middle Euphrates catchment. The Holocene 24, 1351–1368.

Dusar, B., Verstraeten, G., D´Haen, K., Bakker, J., Kapijn, E., Waelkens, M., 2012. Sensitivity of the Eastern Mediterranean geomorphic system iowards environmentla change during the Late Holocene: a chronological perspective. Journal of Quaternary Science 27, 371-382.

Dykoski, C.A., Edwards, R.L., Cheng, H., Yuan, D., Cai, Y., Zhang, M., Lin, Y., Qing, J., An, Z., Revenaugh, J., 2005. A high-resolution, absolute dated Holocene and deglacial Asian monsoon record from Dongge cave, China. Earth and Planetary Science Letters 233, 71-86.

Fuchs, M., 2007. An assessment of human versus climatic impacts on Holocene soil erosion in NE Peloponnese, Greece. Quaternary Research 67, 349–356.

Galbraith R.F., Roberts R.G., Laslett G.M., Yoshida H., Olley J.M., 1999. Optical dating of single and multiple grains of quartz from Jinmium Rock Shelter, northern Australia: Part 1, experimental design and statistical models. *Archaeometry* **41**, 339-364.

Gerasimenko, N., 1997. Environmental and Climatic Chnages between 3 and 5 ka BP in Southeastern Ukraine. In: Dalfes, H.N., Kukla, G., Weiss, H. (Eds.), Third Millennium BC Collapse and Old Word Change. Springer, Berlin, pp. 371-399.

Hofmann R, Müller J, Shatilo L, Videiko, M, Ohlrau R, Rud V, Burdo, N. DalCorso, M., Dreibrodt, S., Kirleis, W., 2019. Governing Tripolye: Integrative architecture in Tripolye settlements. PLoS ONE 14(9): e0222243

Ivanova, 2016. С. В. Иванова. Курганы vs поселения: скотоводы vs земледельцы// Культурные взаимодействия. Динамика и смыслы. Сборник статей в честь 60-летия И.В. Манзуры. Кишинёв: Stratum Plus, 273-291.

ІУМІС, 1972. Історія міст і сіл Української РСР: В 26 т. Черкаська область. Том 24. / Ред. кол. тому: Стешенко О. Л. (гол. редкол.), Гольцев Є. М., Горкун А. І., Дудник О. М., Зайцев М. С., Звєрєв С. М., Зудіна Г. М., Коваленко В. Я., Кузнецов С. М., Курносов Ю. О., Непийвода Ф. М., Степаненко А. О., Тканко О. В. (заст. гол. редкол.), Храбан Г. Ю., Червінський О. А. (відп. секр. редкол.), Шпак В. Т. АН УРСР. Інститут історії. – К.: Голов. ред. УРЕ АН УРСР, 1972. – 788 с.

Kaniewski, D., Paulissen, E., De Laet, V., Waelkens, M., 2008. Late Holocene fire impact and post-fire regeneration from Bereket basin, Taurus Mountains, southwest Turkey. Quaternary Research 70, 228-239.

Kremenetski, C.V., 1997. The Late Holocene Environmental Shift in Russia and Surrounding lands. In: Dalfes, H.N., Kukla, G., Weiss, H. (Eds.), Third Millennium BC Collapse and Old Word Change. Springer, Berlin, pp. 351-370.

Kruts et al., 1981. Круц В.А., Рыжов С.Н. Отчет о работе Тальянковского отряда Трипольской экспедиции в 1981 г. // НА ИА НАНУ, 11б.

Kushtan, 2013. Куштан Д.П. Периодизация и хронология памятников эпохи поздней бронзы Центральной Украины // Проблемы периодизации и хронологии в археологии эпохи раннего металла Восточной Европы: Матер. тематич. науч. конференц. Санкт-Петербург, 4-6 декабря 2013 г. — СПб.: «Скифия-принт», 80-85.

Lang, A., 2003. Phases of soil erosion-derived colluviation in the loess hills of South Germany. Catena 51, 209-221.

Le Roy, M., Deline, P., Carcaillet, J., Schimmelpfennig, I., Ermini, M., 2017. 10Be exposure dating of the timing of Neoglacial glacier advances in the Ecrins-Pelvoux massif, southern French Alps. Quaternary Science Reviews 178, 118-138.

Liritzis, I., Stamoulis, K., Papachristodoulou, C., Ioannides, K., 2013. A re-evaluation of radiation dose-rate conversion factors. *Mediterranean Archaeology and Archaeometry* **13,** 1-15.

Lowe, J.J., Rasmussen, S.O., Björck, S., Hoek, W.Z., Steffensen, J.P., Walker, M.J.C., Yu, Z.C., INTIMATE group, 2008. Synchronisation of palaeoenvironmental events in the North Atlantic region during the Last Termination: a revised protocol recommended by the INTIMATE group. Quaternary Science Reviews 27, 6-17.

Lubos, C.C.M., Dreibrodt, S., Nelle, O., Klamm, M., Friederich, S., Meller, H., Nadeau, J.M., Grootes, P.M., Fuchs, M., Bork, H.-R., 2011. A multi-layered prehistoric settlement structure (tell?) at Niederröblingen, Germany and its implications. Journal of Archaeological Science 38, 1101-1110.

Macklin, M., Benito, G., Gregory, K.J., Johnstone, E., Lewin, J., Michczynska, D.J., Soja, R., Starkel, L., Thorndycraft, V.R., 2006. Past hydrological events reflected in the Holocene fluvial record of Europe. Catena 66, 145-154.

Magny, M., Bégeot, C., Guiot, J., Peyron, O., 2003. Contrasting patterns of hydrological changes in Europe in response to Holocene climate cooling phases. Quaternary Science Reviews 22, 1589-1596.

Magomedov, B.V., Didenko, S.V., 2009. The Cemetery of Chernyakhov Culture by village Legedzino. Excavation in 2008-2009. in: Kruts, V.A., Korvin-Piotrovskiy, A.G., Menotti, F., Ryzhov, S.N., Tolochko, D.V., Chabanyuk, V.V. (Eds.), Talianki - settlement-giant of the Tripolian culture. Investigations in 2009. Kiev, 2009, pp. 56-92.

Migowski, C., Stein, M., Prasad, S., Negendank, J.F.W., Agnon, A., 2006. Holocene climate variability and cultural evolution in the Near East from the Dead Sea sedimentary record. Quaternary Research 66, 421-431.

Murray A.S., Wintle A.G., 2000. Luminescence dating using an improved single-aliquot regenerative-dose protocol. *Radiation Measurements* **32**, 57-73.

Murray A.S., Wintle A.G., 2003. The single aliquot regenerative dose protocol: Potential for improvements in reliability. *Radiation Measurements* **37**, 377-381.

Müller, J., Hofmann, R., Kierleis, W., Dreibrodt, S., Ohlrau, R., Brandtstätter, L., DalCorso, M., Out, W., Rassmann, K., Burdo, N., Videiko, M., 2013. Maidanestke 2013. New excavations at a Tripyllia Mega-site. Studien zur Archäologie in Ostmitteleuropa 16, Habelt, Bonn.

Müller, J., Rassmann, K., Videiko, M., 2016.Trypilla Mega-Sites and European Prehistory 4100–3400 BCE. Routledge Taylor and Francis Group, London.

Neradenko, 2011. Нераденко Т.М. Археологія Черкащини: Посібник-довідник. – Черкаси: Вид. Чабаненко Ю.А., 307.

Ohlrau, R., 2018. *Maidanets'ke. Development and decline of a Trypillian mega-site in Central Ukraine.* PhD Thesis, University of Kiel, Kiel.

Panin, A.V., Fuzeina, J.N., Belyaev, V.R., 2009. Long-term development of Holocene and Pleistocene gullies in the Protva River basin, Central Russia. Geomorphology 108, 71-91.

Pickartz, N., Hofmann, R., Dreibrodt, S., Rassmann, K., Shatilo, L., Ohlrau, R., Wilken, D., Rabbel, W., 2019. Deciphering archeological contexts from the magnetic map: Determination of daub distribution and mass of Chalcolithic house remains. *The Holocene* 29, 1637-1652.

Prasad, S., Brauer, A., Rein, B., Negendank, J.F.W., 2007. Rapid climate change during the early Holocene in Western Europe and Greenland. The Holocene 16 (2), 153–158.

Prescott, J.R., Hutton, J.T., 1994. Cosmic ray contributions to dose rates for luminescence and ESR dating: large depths and long term variations. *Radiation Measurements*, **23**, 497-500.

Rabenhorst, M.C., Schmehling, A., Thompson, J.A., Hirmas, D.R., Graham, R.C., Rossi, A.M., 2014. "Reliability of Soil Color Standards." *Soil Science Society of America Journal* 79, 193–99.

Reimer, P.J., Baillie, M.G.L., Bard, E., Bayliss, A., Beck, J.W., Bertrand, C., Blackwell, P.G., Buck, C.E., Burr, G., Cutler, C.B., Damon, P.E., Edwards, R.L., Fairbanks, R.G., Friedrich, M., Guilderson, T.P., Hughen, K.A., Kromer, B., McCormack, F.G., Manning, S., Bronk Ramsey, C., Reimer, R.W., Remmele, S., Southon, J.R., Stuiver, M., Talamo, S., Taylor, F.W., van der Pflicht, J., Weyhenmeyer, C., 2004. IntCal04 terrestrial radiocarbon age calibration, 26–0 ka BP. Radiocarbon 46, 1029–1058.

Renssen, H., Vandenberghe, J., 2003. Investigation of the relationship between permafrost distribution in NW Europe and extensive winter sea-ice cover in the North Atlantic Ocean during the cold phases of the Last Glaciation. Quaternary Science Reviews 22, 209–223.

Rossato, S., Mozzi, P., 2016. Inferring LGM sedimentary and climatic changes in the southern Eastern Alps foreland through the analysis of a ^{14}C ages database (Brenta megafan, Italy). Quaternary Science Reviews 148, 115-127.

Sanmartín, P., Chorro, E., Vázquez-Nion, D., Miguel Martínez-Verdú, F., Prieto, B., 2014. Conversion of a Digital Camera into a Non-Contact Colorimeter for Use in Stone Cultural Heritage: The Application Case to Spanish Granites. *Measurement* **56**, 194–202.

Schilman, B., Bar-Matthews, M., Almogi-Labin, A., Luz, B., 2001. Global climate instability reflected by Eastern Mediterranean marine records during the late Holocene. *Palaeogeography, Palaeoclimatology, Palaeoecology* 176: 157–176.

Schirrmacher, J., Weinelt, M., Blanz, T., Andersen, N., Salgueiro, E., Schneider, R.R., 2019. Multi-decadal atmospheric and marine climate variability in southern Iberia during the mid- to late-Holocene. Climate of the Past 15, 617-634.

Schumacher, M., Dobos, A., Schier, W., Schütt, B., 2018. Holocene valley incision in the southern Bükk foreland: Climate-human-environment interferences in northern Hungary. Quaternary International, 463, 91-109.

Shidlovsky et al, 2004. Шидловський П.С., Пічкур Є.В., Чорновол Д.К. (2004) Археологічні дослідження поблизу села Аполянка на Уманщині. В Археологічні відкриття в Україні 2002-2003, pp 361-365.

Spurk, M., Leuschner, H.H., Baillie, M.G.L., Briffa, K.R., Friedrich, M., 2002. Depositional frequency of German subfossil oaks: climatically and non-climatically induced fluctuations in the Holocene. The Holocene 12 (6), 707–715.

Staubwasser, M., Weiss, H., 2006. Holocene climate and cultural evolution in late prehistoric-early historic West Asia. Quaternary Research 66, 372-387.

Sycheva, S.A., 2006. Long-term pedolithogenic rhythms in the Holocene. Quaternary International 152-153, 181-191.

Sycheva, S., Glasko, M., Chichagova, O., 2003. Holocene rhythms of soil formation and sedimentation in the Central Russian Upland. Quaternary International 106-107, 203-213.

Terenozhkin, 1961. Тереножкин А.И. Предскифский период на Днепровском Правобережье. — Киев: Изд-во АН УССР, 1961, 248.

Thiel, C., Buylaert, P., Murray, A., Terhorst, B., Hofer, I., Tsukamoto, S., Frechen, M., 2011. Luminescence dating of the Stratzing loess profile (Austria) Testing the potential of an elevated temperature post-IR IRSL protocol. *Quaternary International* **234**, 23–31.

Thornes, J., 2009. Land Degradation. In: Woodward, J. (Ed.), The Physical Geography of the Mediterranean, Oxford University Press, Oxford, pp. 563-581.

Van Andel, T., Zangger, E., Demitrack, A., 1990. Land use and soil erosion in Prehistoric and Historical Greece. Journal of Field Archaeology 17, 379-396.

van Geel, B., Buurman, J., Waterbolk, H.T., 1996. Archaeological and palaeoecological indications of an abrupt climate change in the Netherlands and evidence for climatological teleconnections around 2650 BP. *Journal of Quaternary Science* 11, 451–60.

Vincent, P.J., Lord, T.C., Twelfer, M., Wilson, P., 2010. Early Holocene loessic colluviation in northwest England: new evidence for the 8.2ka event in the terrestrial record? *Boreas* 40, 105–115.

Weiss, H., Bradley, R.S., 2001. What did drive societal collapse? *Science* 291, 609–610.

Weninger, B., Alram-Stern, E., Bauer, E., Clare, L., Danzeglocke, U., Jöris, O., Kubatzki, C., Rollefson, G., Todorova, H., van Andel, T., 2006. Climate forcing due to the 8200 cal yr B.P. event observed at Early Neolithic sites in the Eastern Mediterranean. *Quaternary Research* 66: 401–420.

Wintle A.G., Murray, A.S., 2006. A review of quartz optically stimulated luminescence characteristics and their relevance in single-aliquot regeneration dating protocols. *Radiation Measurements* **41**, 369-391.

Zalizniak et al., 2005. Залізняк Л. Л., Товкайло М. Т., Кухарчук Ю. В. Дослідження стоянок біля с. Добрянка на Черкащині археологічною експедицією НаУКМА у 2001, 2003, 2004 рр.// Маґістеріум. Вип. 20. Археологічні студії / [упоряд.: Л. Л. Залізняк], 6-17.

Zolitschka, B., Negendank, J.F.W., 1998. A high resolution record of Holocene palaeohydrological changes from Lake Holzmaar (Germany). In: Frenzel, B. (Ed.), Palaeohydrology as reflected in lake-level changes as climatic evidence for Holocene times: European Palaeoclimate and Man, vol. 17, pp. 37–52.

Figure captions

Figure 1. Location of the investigation site a) in Eastern Europe, b) the investigation points in the valley of the Talyanki River close to the Tripyllia Giant Settlement Maidanetske (plan of burned houses indicated), and c) simplified chronostratigraphy of the investigated trenches (number on the left side of the columns: MUNSELL color values); data of core 1: Fig. 2a).

Figure 2. Selected laboratory data from a) the long percussion-drilling core 1, b) trench 3 and c) trench 2. Fig. 2 a) TOC- red line, C/N ratio- black line; Fig. 2 c) LOI 500- upper axis, LOI 940- lower axis.

Figure 3. Comparison of the detected Late Quaternary Erosion phases at Maidanetske with the known settlement history, and records of Holocene soil erosion from Russia (Sycheva, 2006, Panin et al., 2009) and Germany (histogram: orange- dated via embedded/ buried archaeological record, green- dated via radiocarbon dating, blue- dated via OSL, Dreibrodt et al., 2010a).

Tables

Table 1 Radiocarbon data

Table 2 OSL data

Table 3 Settlement history of the site (5 km radius) and the region (20 km radius)

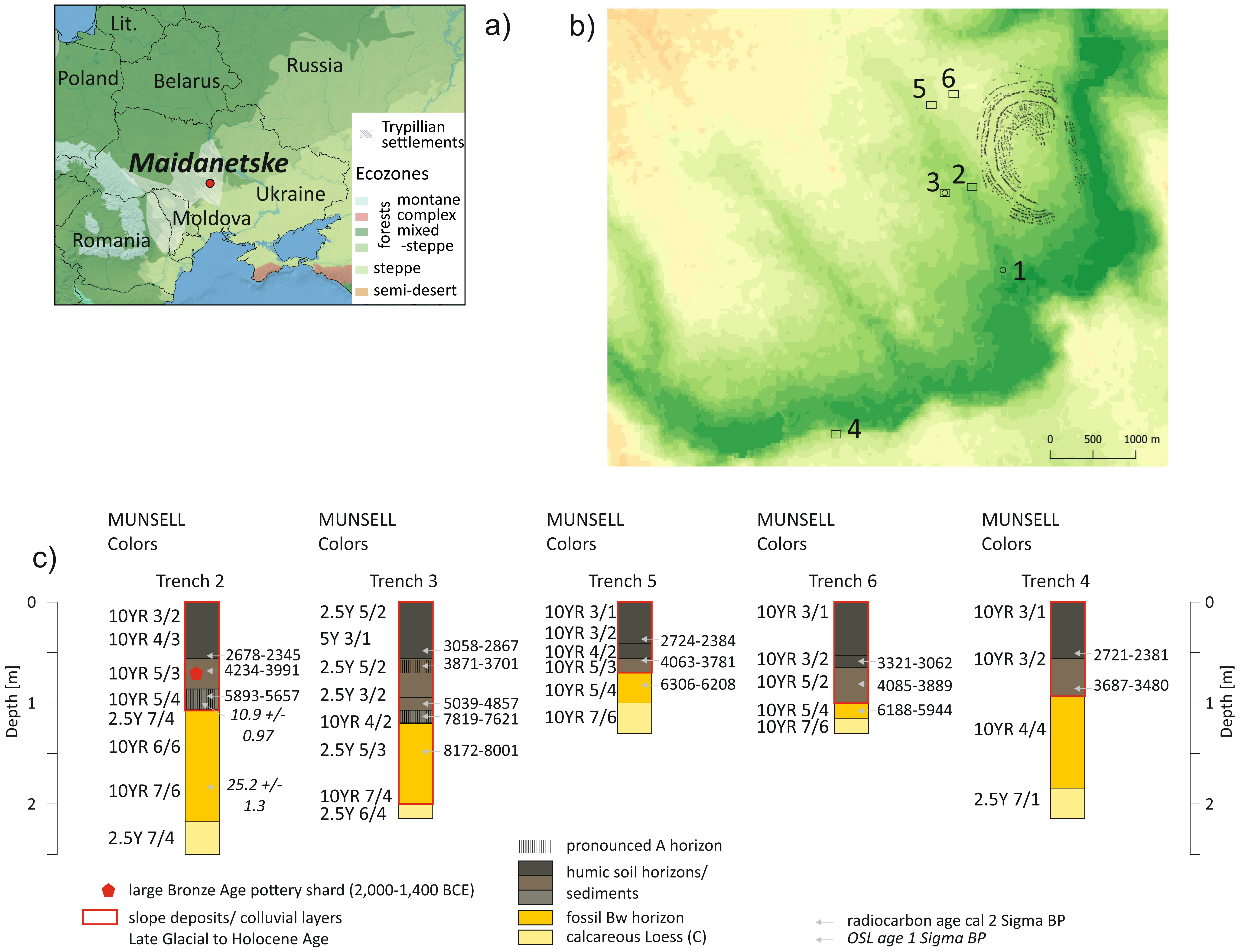
a)
Lit.
Poland
Belarus
Russia
Maidanetske
Ukraine
Moldova
Romania
Trypillian settlements
Ecozones
forests
montane
complex
mixed
-steppe
steppe
semi-desert
b)
1
2
3
4
5
6
0
500
1000 m
c)
MUNSELL Colors
Trench 2
Trench 3
Trench 5
Trench 6
Trench 4
Depth [m]
0
1
2
10YR 3/2
10YR 4/3
10YR 5/3
10YR 5/4
2.5Y 7/4
10YR 6/6
10YR 7/6
2.5Y 7/4
2678-2345
4234-3991
5893-5657
10.9 +/- 0.97
25.2 +/- 1.3
2.5Y 5/2
5Y 3/1
2.5Y 5/2
2.5Y 3/2
10YR 4/2
2.5Y 5/3
10YR 7/4
2.5Y 6/4
3058-2867
3871-3701
5039-4857
7819-7621
8172-8001
10YR 3/1
10YR 3/2
10YR 4/2
10YR 5/3
10YR 5/4
10YR 7/6
2724-2384
4063-3781
6306-6208
10YR 3/1
10YR 3/2
10YR 5/2
10YR 5/4
10YR 7/6
3321-3062
4085-3889
6188-5944
10YR 3/1
10YR 3/2
10YR 4/4
2.5Y 7/1
2721-2381
3687-3480
large Bronze Age pottery shard (2,000-1,400 BCE)
slope deposits/ colluvial layers Late Glacial to Holocene Age
pronounced A horizon
humic soil horizons/ sediments
fossil Bw horizon
calcareous Loess (C)
radiocarbon age cal 2 Sigma BP
OSL age 1 Sigma BP

a)
Stratigraphy
radiocarbon ages (cal 2 Sigma BP)/ OSL ages (1 Sigma ka BP)
Grain Size Distribution (< 2 mm) (%)
MUNSELL COLORS
Color RGB
TOC [% by weight]
C/N (org. matter)
N below detection limits
Medieval/ Modern
Iron Age
4,0 ka BP
EH
YD
Late Glacial aeolian
LGM
M4
M3
fAh M2
M2
fAh M1
M1
S2
Cc (Löss)
S1
911- 735
2426- 2162
2751- 2506
5731- 5608
(charcoal)
3.93±0.1
4438- 4257
5320- 5052
5918- 5750
8.5±0.3
8159- 7878
12030- 11407
12.0±0.4
26.5±0.7
soil Bronze-Iron Age
soil Tripolye-Yamnaya
trees
grasses
Stratigraphy
Loess
slope deposit/ colluvium
A-horizon
Dating
radiocarbon datum
OSL datum
Grain Size [µm]
sand
silt
clay
b)
radiocarbon ages (cal 2 Sigma BP)
Grain Size Distribution (<2mm) [%]
LOI 550/ 940 [% by weight]
sus. mag. LF [10⁻⁵ m³/kg]
MUNSELL COLORS
RGB Colors
Modern to Iron Age
4,0 ka BP
5,0 ka BP
EH
altered by soil formation
Loess
M4
fAh M3
M3
M2
fAh M1
fBw M1
Loess (redeposited?)
3,058- 2,867
3,871- 3,701
5,039- 4,857
7,819- 7,621
8,172- 8,001
c)
radiocarbon ages (cal 2 Sigma BP)/ OSL ages (1 Sigma ka BP)
Grain Size Distribution (< 2 mm) [%]
LOI 550/ 940 [% by weight]
sus. mag LF [10⁻⁵ m³/kg]
MUNSELL COLORS
RGB Colors
Medieval/ Modern
Iron Age
4,0 ka BP
YD
altered by soil formation
Loess Periglacial
M3Ap
M2
M1
S1 fAh
fBw1
fBw2
Cc (Löss)
2,678- 2,345
4,234- 3.991
3,950- 3,350 (potsherd)
5,893- 5,657
10.99 +/- 0.97
27.2 +/- 1.3

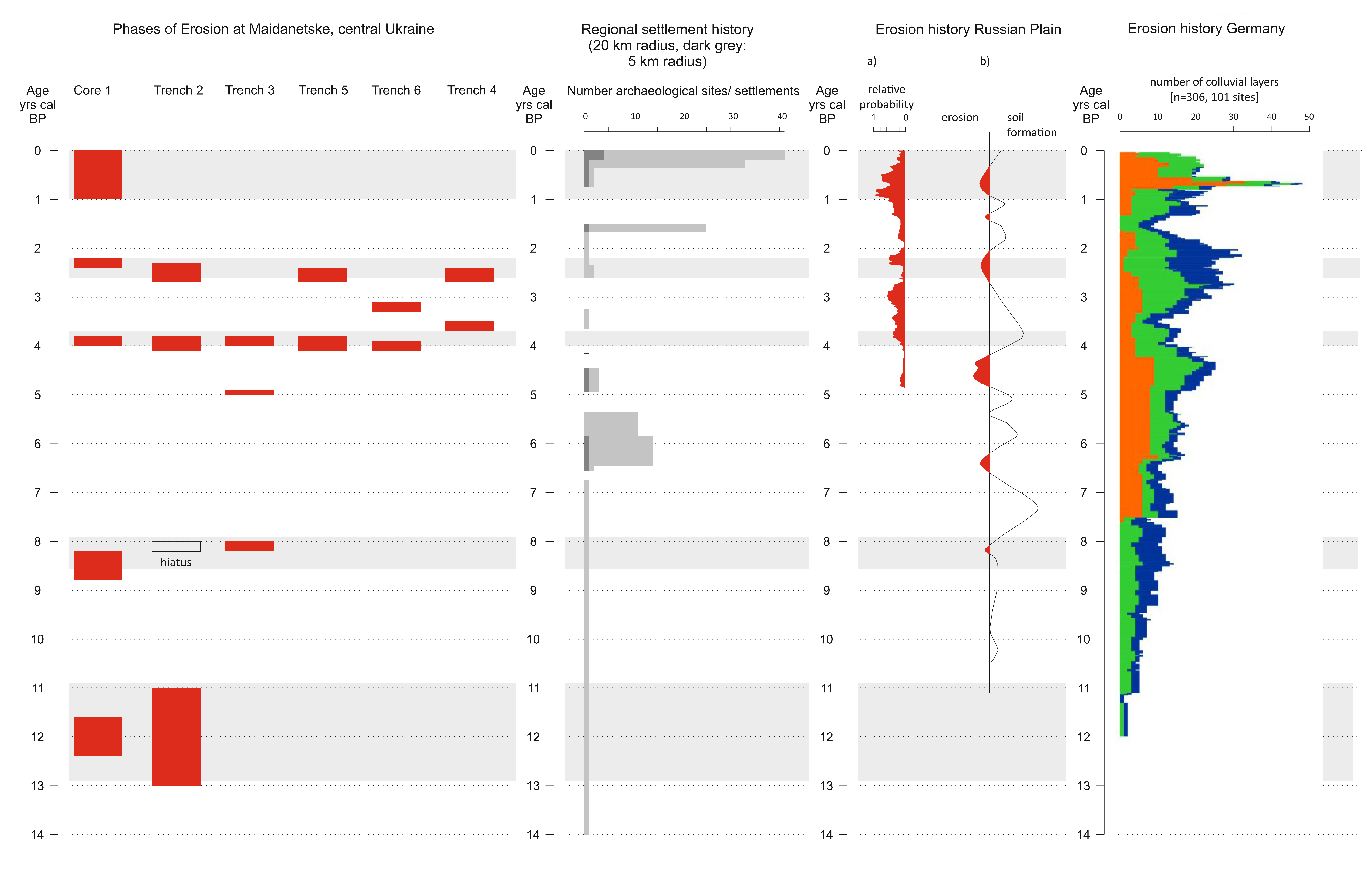

Phases of Erosion at Maidanetske, central Ukraine
Age yrs cal BP
Core 1
Trench 2
Trench 3
Trench 5
Trench 6
Trench 4
hiatus
Regional settlement history (20 km radius, dark grey: 5 km radius)
Number archaeological sites/ settlements
0 10 20 30 40
Erosion history Russian Plain
a)
b)
relative probability
1 0
erosion
soil formation
Erosion history Germany
number of colluvial layers [n=306, 101 sites]
0 10 20 30 40 50
0 1 2 3 4 5 6 7 8 9 10 11 12 13 14

Table 1a Radiocarbon data

Lab	Lab ID	profile	Depth (cm)	radiocarbon age BP	cal 2 Sigma BP	remarks
Kiel	52670	1	340-344	10130±55	12030-11597(86.4%), 11561-11472(6.3%), 11454-11407(2.7%)	Sediment
Kiel	53079	1	323-338	6410±35	7420-7275(95.4%)	Sediment, oulier (krotowina?)
Kiel	53078	1	298-303	7175±55	8159-8087(10.2%), 8069-7931(83.4%), 7893-7878(1.8%)	Sediment
Beta	529991	1	293-298	5100±55	5918-5846(37.2%), 5831-5750(58.2%)	Sediment, Soil formation
Beta	529992	1	288-293	6710±30	7653-7639(1.8%), 7624-7556(75.7%), 7545-7511(17.8%)	Sediment, outlier, too few org. C
Beta	529993	1	283-288	2999±40	3336-3290(7.3%), 3261-3028(87.7%), 3014-3008(0.4%)	Sediment, outlier, too few org. C
Kiel	52669	1	280-284	4550±40	5320-5213(37.1%), 5193-5052(58.3%)	Sediment, Soil formation
Kiel	53077	1	234-239	3927±26	4438-4286(93.0%), 4273-4257(2.4%)	Sediment
Kiel	52667	1	200-204	4949±27	5731-5608(95.4 %)	Charcoal, outlier (redeposition?)
Kiel	53076	1	194-199	2550±24	2751-2698(67.2%), 2635-2617(8.2%), 2591-2537(15.9%), 2531-2506(4.1%)	Sediment, Soil formation
Kiel	52668	1	180-184	2310±40	2426-2392(2.1%), 2382-2302(76.9%), 2246-2178(15.8%), 2171-2162(0.7%)	Sediment
Kiel	53075	1	144-149	895±30	911-735(95.4%)	Sediment
Posznan	62408	2	95-100	5015±35	5893-5805(38.9%), 5796-5781(2.5%), 5774-5657(54.0%)	Sediment, Soil formation
Posznan	62410	2	65-70	3755±30	4234-4198(10.4%), 4184-4070(68.6%), 4045-3991(16.3%)	Sediment
Posznan	62407	2	45-50	2385±30	2678-2667(1.3%), 2656-2644(1.6%), 2492-2345(92.5%)	Sediment
Posznan	113975	3	150-155	7260±40	8172-8001(95.4%)	Sediment
Posznan	113974	3	120-125	6880±40	7819-7814(0.6%), 7796-7621(94.8%)	Sediment, Soil formation
Posznan	113973	3	95-100	4370±30	5039-5005(9.7%), 4981-4857(85.7%)	Sediment
Posznan	113971	3	60-65	3515±30	3871-3701(95.4%)	Sediment, Soil formation
Posznan	113970	3	40-45	2840±30	3058-3049(1.5%), 3040-2867(93.9%)	Sediment

Lab	Lab ID	profile	Depth (cm)	radiocarbon age BP	cal 2 Sigma BCE*/CE**	remarks
Posznan	113547	4	80-90	3345±35	3687-3665(5.2%), 3645-3480(90.2%)	Sediment
Posznan	113546	4	40-60	2475±30	2721-2427(93.6%), 2413-2406(0.6%), 2395-2381(1.3%)	Sediment
Posznan	114060	5	70-80	5460±30	6306-6208(95.4%)	Relict Bw-horizon
Posznan	114059	5	50-60	3595±35	4063-4051(1.0%), 3986-3829(93.9%), 3787-3781(0.5%)	Sediment
Posznan	114058	5	30-40	2480±30	2724-2432(94.6%), 2391-2384(0.5%)	Sediment
Posznan	114064	6	100-110	5290±40	6188-5986(89.4%), 5973-5944(6.0%)	Relict BW-horizon
Posznan	114062	6	70-80	3650±30	4085-3889(95.4%)	Sediment
Posznan	114061	6	50-60	2980±30	3321-3309(1.1%), 3247-3062*(94.3%)	Sediment

Table 1 b OSL data

Lab	Lab ID	profile	Depth (cm)	Water content (%)	OSL grain size (µm)	U (ppm)	Th (ppm)	K (%)	D* (Gy/ka)	De (Gy)	OSL age (ka)
Szeged	1504	1	465	20±5	11-20	2.77±0.02	10.03±0.15	1.63±0.04	2.61±0.06	69.47±0.81	26.5±0.7
Szeged	1505	1	380	19±5	11-20	2.98±0.03	9.23±0.16	1.89±0.06	2.86±0.07	34.68±0.67	12.0±0.4
Szeged	1506	1	295	17±5	11-20	2.98±0.03	9.76±0.16	1.87±0.05	2.94±0.07	25.30±0.41	8.5±0.3
Szeged	1507	1	210	19±5	11-20	2.95±0.03	10.09±0.15	1.68±0.04	2.76±0.06	10.84±0.09	3.93±0.1

Lab	Lab.-Nr.	profile	Depth (cm)	^{238}U (ppm)	^{232}Th (ppm)	^{40}K (ppm)	D* (Gy/ka)	De (Gy), aliquots	OSL age (ka)
Gdynia	GdTL-1892	2	180	29.14±0.74	42.5±0.12	498±33	2.54±0.11	69.2±1.4	27.2±1.3
Gdynia	GdTL-1893	2	100	24.30±0.70	40.5±0.12	576±40	2.53±0.12	28.0±2.0	10.99±0.97

Period	Numerical age (BCE*/CE**//BP)	Archaeological sites in the micro-region bold = 5 km radius, black =20 km radius, grey = 20 km, no precise dating available	"material-culture"	Reference
Palaeolithic	Lower …//until 150,000	-		
	Middle …//until 35,000	-		
	Upper …//until 9,950	Gordashovka, Lashova		Shidlovsky et al., 2004: 364
Mesolithic	8,000– 6,000*// 9,950- 7,950	Dobryanka 1	Kukrek	Neradenko, 2011 Zalizniak et al., 2005
Neolithic	6,000– 4,800*// 7,950- 6,750	Dobryanka 3	Buh-Dniester culture	Zalizniak et al., 2005
Chalcolithic	Early (Tripolye A) 4,600 –4,500*// 6,550- 6,450	**Grebenukiv Yar**, Romanovka	Tripolye	
	Middle (Tripolye B) 4,500-3,900*// 6,450- 5,850	Onoprievka, Vesely Kut, Gordashovka 1, Hlybochok, Rozsohovatka, Kolodyste 1, Krivi kolina, Pischana, Sverdlikove, Nebelivka	Tripolye	
	Late (Tripolye C) 3,900-3,400*// 5,850- 5,350	**Maidanetske,** Kobrinovo, Romanovka, Moshurov 1, Moshurov 2, Moshurov 3, Gordashovka 2, Talne 1, 2 and 3, Rohy, Talianki, Kamyaneche, Kolodyste	Tripolye	
Bronze Age	Early Bronze Age 3,000– 2,500*// 4,950- 4,450	Kurgans close to **Maidanetske,** Legedzyne, Dobrovody, settlement Maidanetske (Shirokiy bereg), Belashki "Oksanichev yar", Vishnopil, Talne (3), Rohy, Moshurov	Yamnaya culture, kurgans	Отчеты, Иванова, 2016: 273-290; Kruts et al., 1981: 4
	Middle Bronze Age 2,600– 2,200*// 4,550- 4,150	-		
	Transitional period 2,200– 1,700*// 4,150- 3,650	M**aidanetske (?)**		
	Late Bronze Age 1,700– 1,300*// 3,650- 3,250	Legedzyne 2		Magomedov and Didenko, 2009: 56; Куштан, 2013: 84
	Final Bronze Age 1,300– 900*// 3,250- 2,850	-		
Early Iron Age	Pre Scythian time 9th– mid 7th c.*// 2,750- 2,600	No settlements		Terenozkin, 1961

	Scythian time mid 7th– 3rd c.*// 2,600- 2,350	Kurgans close to Legedzyne, Kolodiste Belashki, Moshurov (settlements)- „early iron age“	Scythian, kurgans	Kruts et al., 1981: 4.
	Sarmat time 3rd- 2nd c.*– 4th c.**//2,350- 1,550	Kurgan in Kolodiste		
Late Roman time	mid 3rd- first half 5th c.**// 1,700- 1,500	**Maidanetske,** Legedgzyne 1 and 2, Legedzyne graveyard, Sverdlikove (burials), Kobrinovo, Belashki (4), Glibochok 1 and 2, Vesely Kut, Potash, Papuzentci, Pavlivka 1, Zelenkiv, Gordashivka 1, 2 and 3, Vishnopil (2), Talne, Rohy, Oksanine 1 and 2, Kolodiste	Chernyakhov culture	Magomedov and Didenko, 2009: 56; Kruts et al., 1981: 4
Middle Ages	Early middle Age 5th-10th c.**// 1,450- 950	Moshurov, Pishana (Penkovska culture)		
	High Middle Ages 10th c.-1250**// 950- 750	-		
	Late middle age 1250- 1500**// 750- 450	1/1 villages		ІУМІС, 1972
Early modern period	1500- 1750**// 450- 200	1/33 villages		ІУМІС, 1972
Late modern period	since 1750**// since 200	1/41 villages At the end of the 19th c. a sugar factory was built in Maidanetske, in action until the end of the 20th century. Construction of cascade ponds.		ІУМІС, 1972